Wooden Stud Walls with Aerogel Thermal Insulation—Material Properties and HAM Simulations

Axel Berge **Carl-Eric Hagentoft, PhD** **Paula Wahlgren, PhD**

ABSTRACT

This study evaluates the heat and moisture performance of wooden stud walls with aerogel blankets as the main insulation. There is always a risk that a new material will create problems if it is applied in the same way as conventional materials. To predict and prevent such problems, it is of essential interest to analyze aerogel applications from a heat and moisture perspective. In this study, thermal conductivity and the vapor diffusivity of aerogel blankets were measured. The work found that the aerogel blankets can be compressed and that compression actually lowers the thermal conductivity. The measured results were used as input in numerical simulations. Four different wall layouts were modeled and compared to a wall with conventional insulation. The simulations showed that the thickness of a wooden stud wall could be decreased to 60% with aerogel blankets instead of conventional insulation, with the same thermal transmittance. Also, the position of the aerogel layers had a large influence on the moisture condition in the wall. The aerogel wall in the study with the best moisture performance has a homogeneous aerogel layer outside of the wooden studs and the studs are in line, forming a continuous thermal bridge through the wall. The moisture performance of the best aerogel wall in the study was as good as the studied wall with conventional insulation.

INTRODUCTION

Today there is a lot of concern regarding how humans affect the environment. One large source of impact on the environment is energy production; therefore, a large effort is made to lower the energy consumption through all of society. The Swedish Government (2013) aims to decrease energy consumption by 20% until the year 2020; similar goals can be seen throughout Europe.

The environmental concern has led to new concepts to lower the energy consumption of new buildings. One of the main factors for energy loss in buildings is the heat transmission through the building walls. On one hand, the thermal transmittance (U-factor) of a wall can be decreased by adding new layers of insulating materials, thus decreasing the heat losses. On the other hand, the wall thickness will increase, which reduces the available building area, which may lead to architectural problems such as decreased natural lightning. A change in wall layout will also lead to a change in the moisture conditions in the wall. Therefore, the moisture performance of a new wall should be evaluated to reveal any risks of moisture damage such as mold or rot.

During the last century, some new insulation materials have been developed with thermal properties superior to those of conventional insulation materials (Berge and Johansson 2012). One of these materials is aerogel, invented by Kistler (1931) during the thirties. An aerogel is a former gel which has been dried at supercritical conditions so that the original gel structure is kept intact. This can lead to a material with high porosity and a pore diameter in the range of 20–40 nm ($1 \cdot 10^{-6}$–$2 \cdot 10^{-6}$ in.) (Soleimani Dorcheh et al. 2008). The pore diameter is of the same magnitude as the mean free path of air, where the mean free path is the average length a gas molecule travels before colliding with another gas molecule. This leads to a decreased probability of gas-gas collisions compared to gas-solid collisions. Gas-solid collisions transfer less energy than gas-gas collisions, which leads to a situation where an air-filled

Axel Berge *is a doctoral student,* ***Carl-Eric Hagentoft*** *is a full professor, and* ***Paula Wahlgren*** *is a senior lecturer in the Division of Building Technology, Department of Civil and Environmental Engineering, Chalmers University of Technology, Göteborg, Sweden.*

porous material can have a lower conductivity than still air with unlimited space. This has been shown by Fricke et al. (1992), who found a thermal conductivity for aerogel as low as 13 m·W/m/K (0.083 Btu·in./h/ft^2/°F), which is substantially lower than the conductivity of example mineral wool or expanded polystyrene insulation with a conductivity above 30 m·W/m/K (0.21 Btu in./h/ft^2/°F).

A problem with monolithic aerogels is that they are very fragile, which creates issues with handling the material. This has led to the creation of aerogel composites, where some kind of reinforcement fibers are mixed with the gel before drying (Stepanian et al. 2006). One type of composite is the so-called aerogel blanket, shown in Figure 1, which can be stored in rolls and can be handled like a thick fabric.

Today aerogel blankets are very expensive compared to other insulation materials, but the price is decreasing and has been forecast to decrease even more in the future. Therefore, it is of interest to find the benefits that a low thermal conductivity could yield and to investigate possible problems that could occur.

Aim

This work aims to investigate aerogel blankets as a possible insulation material for walls. The work has been divided into two parts: the first part is an analysis of the material properties to understand the material and the second part is numerical simulations of heat and moisture conditions in a load-bearing wooden stud wall element. This work generates the first insight into possible benefits from using aerogel blankets as the primary insulation in wooden stud walls.

Figure 1 *A roll of aerogel blanket with a nominal thickness of 10 mm (0.39 in.).*

MATERIAL PROPERTIES OF AEROGEL BLANKETS

To simulate the use of aerogel blankets in a wall structure, various material properties have to be known to use as input data in the model. For this study, the most important properties are those related to heat and moisture transport. One problem with determining the properties is the variation through the specimens. Since aerogel is a fragile material, the aerogel in the outer layers of the blanket will break and fall off as dust, leaving only reinforcement fibers. Deeper into the material, the fiber reinforcement keeps the aerogel matrix together. For simulation input you have to choose between apparent properties, representing the whole material piece, or you have to try to measure the properties of the different layers of the specimen.

The measurements were focused on one type of aerogel blanket with a low thermal conductivity. The results were compared to another aerogel blanket covered with a dust protection coating. The coating consisted of some kind of polymer applied to the surface of the blanket to stop aerogel particles from falling off. The properties of the blankets differ to some extent, and while no clear conclusions about the effect of adding a dust coating can be drawn, it can give indications. Some basic properties of the aerogel blankets are shown in Table 1. The specimen thickness was measured according to EN 823, *Thermal insulation products for building applications – determination of thickness* (CEN 1994).

Thermal Conductivity Measurements of Aerogel Blankets

The thermal conductivity was measured in a guarded heat flowmeter apparatus. A 300 × 300 mm^2 (11.8 × 11.8 in.^{2}) large sample was put in between two plates with different temperatures. To decrease the measurement error from the sample thickness, three layers of aerogel blanket, stacked on top of each other, were measured corresponding to a total nominal thickness of 30 mm (1.18 in.). A heat flowmeter measured the heat flow from the hot plate into the material, through the middle 100 × 100 mm^2 (3.94 in.^{2}) part of the sample. Spacers were used to lock the sample thickness during the measurement. With the area, A, temperature difference, ΔT, heat

Table 1. Density and Thickness of Two Types of Aerogel Blanket Without (A) and With (B) a Dust Coating

Sample	Density, ρ		Measured Thickness, t		Nominal Thickness, t_{nom}	
	kg/m^3	lb/ft^3	mm	in.	mm	in.
A	157	9.81	10.6	0.413	10	0.394
B	147	9.19	10.2	0.401	10	0.394

flow, Q, and thickness, d, the thermal conductivity, λ, can be calculated from Equation 1.

$$\lambda = \frac{Q \cdot d}{A \cdot \Delta T} \quad (1)$$

Temperature Dependence of the Thermal Conductivity. Thermal conductivity measurements were performed at different mean temperatures, from 10°C to 40°C (50°F to 104°F), to examine the variation in thermal conductivity due to temperature. The results for blanket type A are shown in Figure 2, which gives an average conductivity of 15.4 m·W/m/K (0.107 Btu·in./h/ft^2/°F) at 10°C (50°F) and a temperature variation for each degree of 0.02 (m·W/m/K)/K ($8 \cdot 10^{-5}$ [Btu·in./h/ft^2/°F]/°F). The temperature influence on the thermal conductivity is quite small and can probably be neglected in a wall context. The result can be compared to the results by Pietruszka et al. (2012), who measured a thermal conductivity of aerogel blankets between 15.0 and 16.6 m·W/m/K (0.104 and 0.115 Btu·in./h/ft^2/°F) at 10°C (50°F).

The thermal conductivity of the dust-coated aerogel blanket (B) was also measured; it gave a resulting thermal conductivity of 19 m·W/m/K (0.13 Btu·in./h/ft^2/°F) at 10°C (50°F). This is much higher than the aerogel blanket without the coating, but it is not the same product so it cannot be compared directly.

Compression Dependence of the Thermal Conductivity. Aerogel is a fragile material, held together by the reinforcement fibers. On the surface of the material, the fibers cannot entangle the aerogel as much as in the core, therefore aerogel falls off as dust, leaving a surface layer with less aerogel and more air. Since the aerogel itself has a lower conductivity than still air, a compression of the specimen might decrease the measured conductivity by reducing the air-filled outer layers.

From the product technical guide for the aerogel blankets, the measured conductivity is 13.1 m·W/m/K for a sample compressed to 83% of the nominal thickness. To test the influence of thickness, three specimens of aerogel blanket were tested at a mean temperature of 10°C (50°F). The maximum thickness was approximately 32 mm (1.26 in.) and the minimum thickness was limited to approximately 29 mm (1.14 in.) by the possible compression in the metering equipment. The thermal conductivity of each specimen was measured at several different thicknesses, from the minimum thickness up to the measured sample thickness.

The results are shown in Figures 3 and 4 (in SI and I-P units, respectively), where it is shown that 10% compression gives 1 m·W/m/K (0.06 Btu·in./h/ft^2/°F) lower thermal conductivity. Figures 3 and 4 also show the conductance through the whole thickness of the specimen. The conductance is defined as the heat flow through the material layer, normalized over area and temperature. Even though the thermal conductivity decreases with a lower thickness, the total flow still increases,

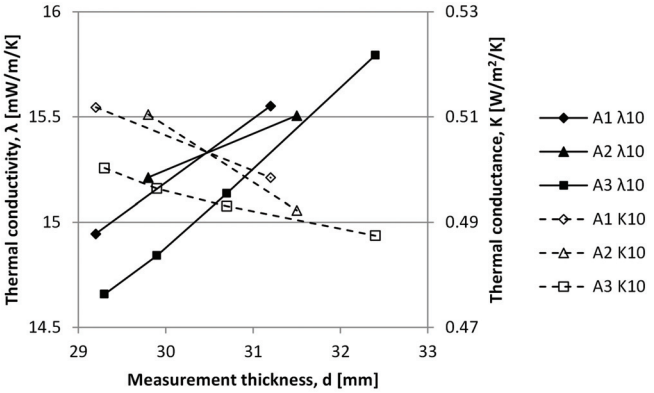

Figure 3 *Thermal conductivity and thermal conductance of samples A1–A3 as a function of the sample compression represented by the measured thickness (SI units).*

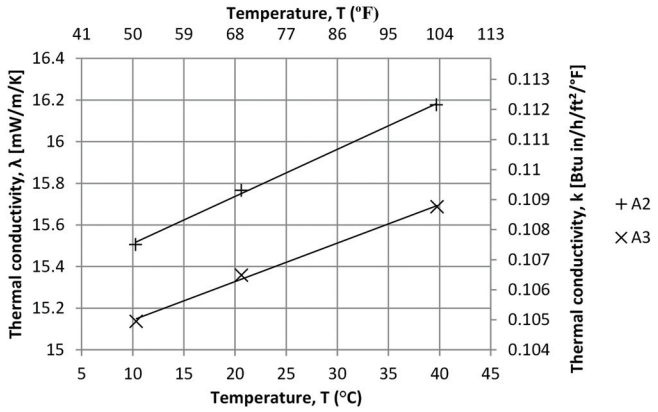

Figure 2 *Thermal conductivity of aerogel blankets as a function of temperature for two different specimens of the same type.*

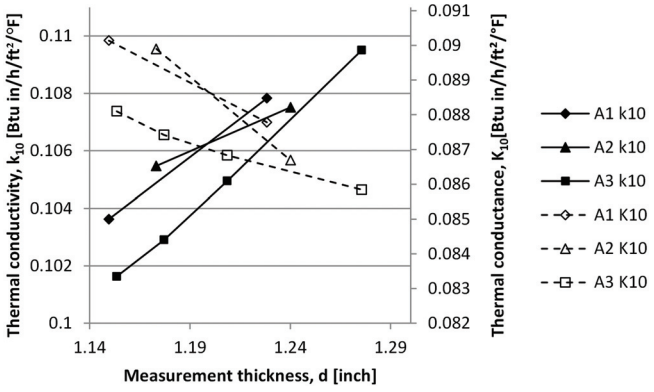

Figure 4 *Thermal conductivity and thermal conductance of samples A1–A3 as a function of the sample compression represented by the measured thickness (I-P units).*

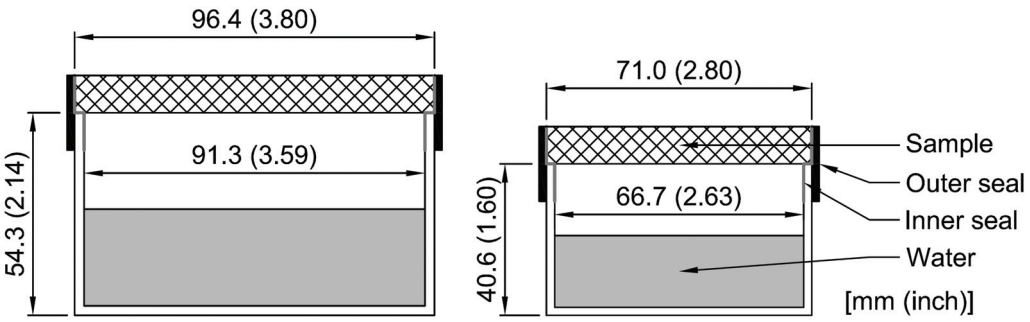

Figure 5 *Set-up for wet cup measurements. The cups are cylindrical.*

which means that an uncompressed aerogel blanket still gives a higher thermal resistance per invested dollar.

Vapor Diffusion Coefficient for Aerogel Blankets

The vapor diffusion properties of the aerogel blankets were measured by the cup method. Samples of aerogel blanket were mounted on a glass cup half filled with water. The samples were placed in a climate chamber at 20°C (68°F) and 50% relative humidity (RH). The samples were continuously weighed, and with the weights together with the measured time, the mass flow of vapor leaving through the sample could be calculated.

To analyze the possible increased flow through the cut circumference of the samples, two different sample sizes where tested. The two sample sizes had different relations between the area and the circumference so that a quotient of flow per edge length could be calculated.

The setups for the measurements are shown in Figure 5. The vapor diffusivity can then be calculated from Equation 2. From the diffusivity, the permeability can be calculated using Equation 3.

$$G = \frac{\Delta\varphi \cdot v_s \cdot A}{\frac{d_a}{D_{v,\,a}} + \frac{d_{aeb}}{D_{v,\,aeb}}} \tag{2}$$

$$\delta_v = \frac{\Delta\varphi \cdot v_s}{\Delta P_v} \cdot D_v \tag{3}$$

where

G	=	mass flow, kg/s (lb/h)
$\Delta\varphi$	=	difference in relative humidity, dimensionless
v_s	=	saturation vapor content, kg/m^3 (lb/ft^3)
A	=	sample area, m^2 (ft^2)
d_a , d_{aeb}	=	air gap thickness and aerogel sample thickness, respectively, m (in.)
$D_{v,a}$, $D_{v,aeb}$	=	vapor diffusivity of air and aerogel, respectively, m^2/s
δ_v	=	vapor permeability, kg/Pa/s/m (perm in.)
ΔP	=	difference in partial pressure, Pa (mm Hg)

Table 2. Measurement of Permeability on Small and Large Samples of Aerogel Blanket, Without (A) and With (B) a Dust Coating

Sample	Diffusivity, D_v, $\cdot 10^{-6}$ m^2/s	Permeability, δ_v	
		$\cdot 10^{-12}$ kg/Pa/s/m	Perm in.
A1 small	5.93	45	30.7
A2 small	5.54	42	28.6
A3 small	5.12	38	26.5
A_{avg} large	5.53	42	28.6
A4 large	5.32	40	27.5
A5 large	5.15	39	26.6
A6 large	5.67	43	29.3
A_{avg} large	5.38	40	27.8
$A_{tot.avg}$	5.46	41	28.2
B1 large	6.32	48	32.7
B2 large	6.61	50	34.2
B3 large	5.78	43	29.9
B_{avg}	6.24	47	32.2

The results from the measurements are shown in Table 2. The variation between the different sample sizes is of the same magnitude as the variation between samples of the same size, which indicates that the extra vapor flow through the edge is small compared to the total vapor flow through the sample. This gives an average permeability of $5.46 \cdot 10^{-6}$ m^2/s (28.2 perm in.).

The influence from a dust coating was also tested. The coated blanket (B) was of another type, with a higher thermal conductivity, but the results could indicate influence of a coating. The measurement showed that the coated samples had a higher permeability than the samples without the coating. This indicates that the type of coating used does not interrupt the vapor flow through the material. It can be assumed that it would be possible to coat the other aerogel blanket (A) with

the same coating without any large influence on the moisture transport through the wall.

WALL ASSEMBLY SIMULATIONS

A common Swedish concept of a wall for low-energy buildings with conventional insulation was found from an insulation material producer and is shown as walls 1a and 1b in Figure 6. From the interior, the layers of the structure are:

- 13 mm (1/2 in.) gypsum board
- 45 mm (1.77 in.) layer for service penetrations with mineral wool and wooden studs
- vaportight film
- homogenous layer of mineral wool
- load-bearing layer with mineral wool and wooden studs
- homogenous mineral wool board
- 25 mm (0.99 in.) ventilated air gap
- wooden façade

The load-bearing studs are 120×45 mm^2 (4.73×1.77 in.^{2}) with a center distance of 600 mm (1.97 ft). This is based on the design load from snow on a 15 m (49 ft) wide roof placed in Göteborg, Sweden (Johannesson 1992).

When a wall gets thinner, the influence of the thermal bridge through structural elements increases. Therefore, two different placements of the wooden studs were analyzed: alternating as in the "a" cases or in line as in the "b" cases, shown in Figure 6. Walls 1a and 1b are the reference walls with conventional insulation materials. These are compared to two versions of aerogel walls with the same U-factor; wall type 2, where a homogenous aerogel layer is placed in between the layer for service penetrations and the load-bearing layer, and wall type 3, where a homogenous aerogel layer is placed on the outside of the construction, before the façade.

Thermal Analysis of the Wall Assemblies. The heat flows through the wall assemblies were simulated with the Heat Transfer Module of COMSOL Multiphysics® 4.2b (COMSOL 2013), a finite element method software, with constant bound-

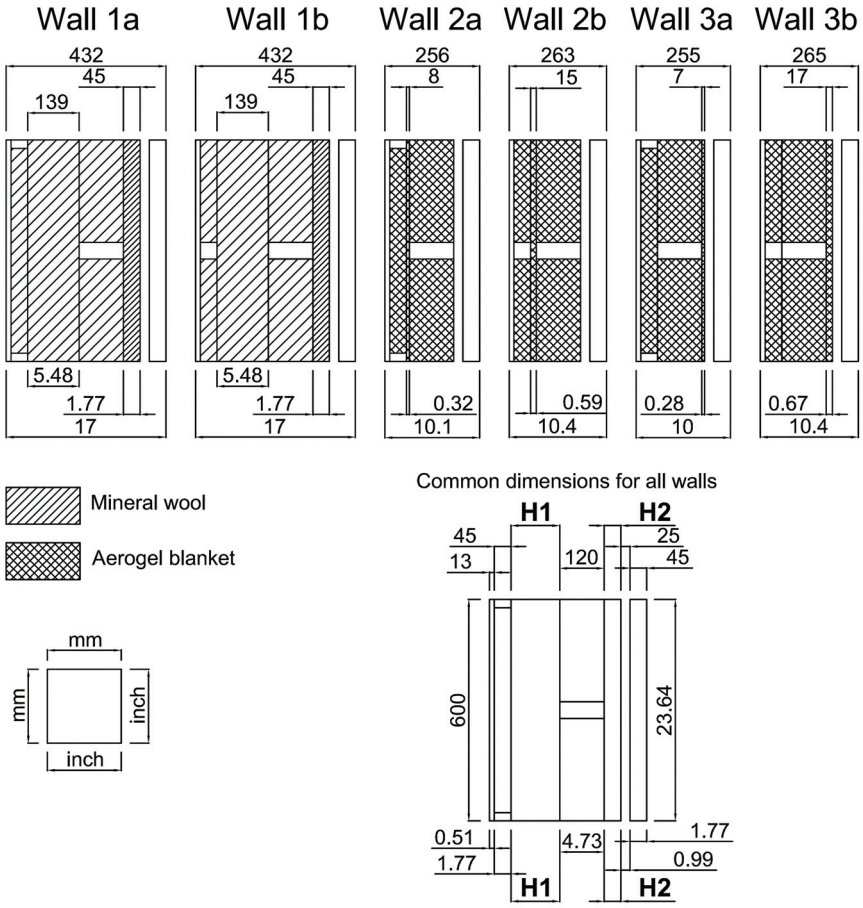

Figure 6 *Horizontal incisions of the insulated wall constructions. Walls 1a and 1b are insulated with conventional insulation and walls 2a, 2b, 3a, and 3b with aerogel blanket insulation. The wall to the bottom right shows the dimensions common for all walls, such as the load-bearing layer, and also the position of the two layers H1 and H2, for which the thickness was varied in the thermal analysis. The measures up and to the left are in millimeters and the measures down and to the right are in inches.*

ary temperatures. The U-factor was calculated and the thickness was altered until each wall had a U-factor of 0.100 W/m^2/K (0.0176 Btu/h/ft^2/°F) to represent a modern low-energy building. The thickness was varied for layer H1 for walls 1a, 1b, 2a, and 2b and for layer H2 for walls 3a and 3b. The positions of layers H1 and H2 are shown in the bottom right of Figure 6.

For the choice of walls, similarity in U-factor was prioritized rather than actual available material dimensions. Therefore, the adjusted homogenous layers have unconventional thicknesses.

The input data for the thermal analysis is shown in Table 3 and were taken from the material database in the simulation software WUFI 2D (IBP 2013), which was used for the moisture analysis. The air gap and the façade were treated as an extra resistance of 0.20 m^2·K/W (1.14 ft^2·h·°F/Btu) added to the exterior surface resistance. This gave internal and external heat transfer coefficients of 25 and 3 W/m^2/K (4.4 and 0.53 Btu/h/ft^2/°F), respectively (Petersson 2009).

The resulting wall thicknesses are shown in Table 4 together with the relative thickness compared to wall 1. With aerogel blanket insulation, the total wall thickness could be reduced to 60% of the original thickness for the same U-factor. For both the conventional walls and the aerogel blanket walls, the influence of the relative position of studs is small. For the conventional wall the position did not affect the thickness at all, and for the aerogel walls the thickness changed a maximum of 10 mm (0.39 in.), which correspond to a difference of around 4%.

Table 3. Thermal Conductivities Used for the Thermal Analysis of the Wall Assemblies

Material	Thermal Conductivity	
	m·W/m/K	Btu·in./h/ft^2/°F
Gypsum board	200	1.39
Mineral wool	36	0.25
Wooden studs	90	0.62
Mineral wool board	33	0.23
Aerogel blankets	15.4	0.107

Table 4. Simulated Wall Thickness and Relative Thickness Compared to Wall 1

Wall	Total Wall Thickness, *t*		Thickness Relative to Wall 1 (%)
	mm	in.	
1a	432	17.0	100.0
1b	432	17.0	100.0
2a	256	10.1	59.3
2b	263	10.4	60.9
3a	255	10.0	59.0
3b	265	10.4	61.3

Moisture Performance Analysis. The wall constructions were analyzed in a combined heat and moisture simulation in WUFI 2D (IBP 2013). The outdoor climate was varied over a repeated year of climate data for Göteborg, Sweden. The indoor climate was based on Standard EN 13788 (CEN 2012), one of the possible climate inputs in WUFI 2D (Zirkelbach et al. 2013). This gave an indoor temperature of 22°C (72°F) and an indoor moisture load of 4 g/m^3 (0.23 gr/gal) for outdoor temperatures below 0°C (32°F), decreasing linearly with temperature to zero at 20°C (68°F). The vaportight film, placed after the service gap in the walls, was chosen to have an equivalent air diffusion layer thickness of 1500 m (4900 ft).

The daily average temperature and relative humidity in the wall were monitored at eight different points, shown in Figure 7. From the temperature, the critical relative humidity for the wood elements was calculated according to Huuka and Viitanen (2009) and the mold growth potential was calculated as the quotient between the relative humidity and the critical relative humidity. Thus, a higher value indicates worse moisture conditions and a value above 1 indicates a risk of mold growth.

The results from the simulations are shown in Table 5. Walls 2a and 2b are the only walls for which the mold growth

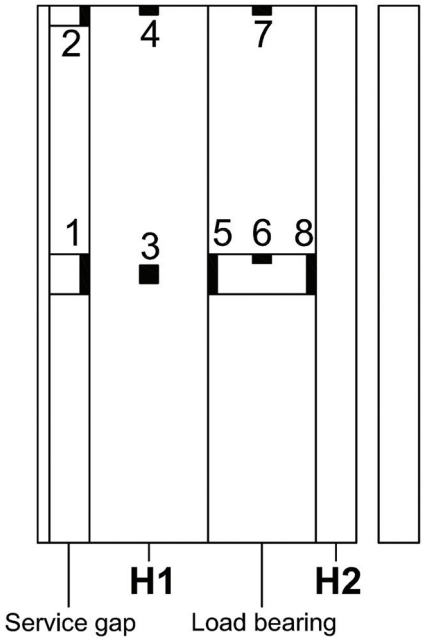

Figure 7 *The eight measurement positions in the heat and moisture simulations for the analyzed walls. This is a schematic version of the walls in Figure 6. The measurement points on the wooden studs were measured on the surface of the studs. Walls 3a and 3b do not have the layer H1, which is why there are no results for positions 3 and 4.*

Table 5. Resulting Minimum and Maximum Values for the Mold Growth Potential and the Relative Humidity for the Different Positions in the Analyzed Walls

	Wall Position							
	1	**2**	**3**	**4**	**5**	**6**	**7**	**8**
				Wall 1a				
MP_{max}, dimensionless	0.74	0.71	0.74	0.75	0.79	0.82	0.85	0.92
MP_{min}, dimensionless	0.56	0.56	0.31	0.28	0.45	0.51	0.43	0.47
RH_{max}, %	60	57	60	60	63	65	68	75
RH_{min}, %	45	45	25	22	36	41	35	39
				Wall 1b				
MP_{max}, dimensionless	0.71	0.74	0.74	0.75	0.78	0.82	0.85	0.92
MP_{min}, dimensionless	0.56	0.56	0.30	0.28	0.45	0.51	0.44	0.47
RH_{max}, %	57	59	59	60	63	65	68	75
RH_{min}, %	45	44	24	23	36	41	35	39
				Wall 2a				
MP_{max}, dimensionless	0.93	0.72	0.72	0.75	0.74	0.82	0.84	1.03
MP_{min}, dimensionless	0.68	0.59	0.46	0.28	0.49	0.59	0.48	0.41
$MP > 1$, d	—	—	—	—	—	—	—	7 (3)[1]
RH_{max}, %	75	58	58	60	59	65	67	85
RH_{min}, %	54	47	37	22	40	48	39	36
				Wall 2b				
MP_{max}, dimensionless	0.74	0.77	0.71	0.76	0.73	0.81	0.85	1.02
MP_{min}, dimensionless	0.62	0.62	0.40	0.34	0.47	0.58	0.50	0.41
$MP > 1$, d	—	—	—	—	—	—	—	6 (3)[1]
RH_{max}, %	59	62	57	61	59	65	68	84
RH_{min}, %	50	49	32	27	38	47	41	36
				Wall 3a				
MP_{max}, dimensionless	0.96	0.72	—	—	0.69	0.78	0.82	0.95
MP_{min}, dimensionless	0.69	0.59	—	—	0.47	0.55	0.47	0.42
RH_{max}, %	77	58	—	—	55	62	66	77
RH_{min}, %	55	47	—	—	38	44	38	37
				Wall 3b				
MP_{max}, dimensionless	0.74	0.77	—	—	0.65	0.74	0.82	0.88
MP_{min}, dimensionless	0.63	0.61	—	—	0.38	0.47	0.48	0.40
RH_{max}, %	59	62	—	—	52	59	65	70
RH_{min}, %	50	49	—	—	30	38	39	35

[1]Described as *x (y)* where *x* is the total number of days and *y* is the longest sequence of consecutive days.

potential exceeds 1—it occurs for 7 days and 6 days, respectively, with a maximum of 3 consecutive days for both walls. This occurs at position 8, which for these walls is next to the ventilated cavity behind the façade and thus close to outdoor conditions. For the outdoor climate the mold growth potential is more than 1 during 49 days of the year, with a maximum of 7 consecutive days. Therefore, outdoor wood is usually treated against moisture damage and requires more maintenance than wood inside the walls.

The mold growth potential maximums are visualized in Figure 8. Both the various walls and the different data collection positions are shown.

Walls 2a and 3a characterize themselves with a high mold growth potential maximum in position 1, close to the indoor condition. In these walls, the wooden studs are positioned alternately and, therefore, heat is let out from the point through the load-bearing wooden stud while the indoor heat is stopped by an aerogel layer. The temperature at the point decreases and consequently the relative humidity goes up. A higher indoor moisture load would increase the mold growth potential, possibly above 1.

Position 8 seems to be the worst position for all walls except wall 3a, where positions 1 and 8 have almost the same maximum. It is in position 8 that walls 2a and 2b exceed the mold growth potential limit of 1.

Wall 3b is the aerogel wall with the best moisture performance in the simulations. Compared to the conventional walls, walls 1a and 1b, the mold growth potential maximum in the outer parts of the wall is lower for wall 3b but higher in the inner parts of the wall. Though, as for walls 1a and 1b, the mold growth potential is far below 1 in all positions of wall 3b.

CONCLUSION

For aerogel blankets, the apparent thermal conductivity increases with thickness. This means that a compressed blanket has a better thermal conductivity. On the other hand, the total resistance of a blanket also decreases with compression and, consequently, an uncompressed blanket has a higher thermal resistance relative to the material cost. To model a wall assembly with aerogel you would have to describe how the blankets are simulated, compressed or noncompressed.

From a pure thermal analysis of the aerogel blankets, the wall thickness of the studied load-bearing wooden stud walls could be decreased by around 60% by using aerogel blanket insulation instead of conventional insulation. The comparisons were made for a wall with a U-factor of 0.100 W/m^2/K (0.0176 Btu/h/ft^2/°F) with 120 × 45 mm^2 (4.7 × 1.8 in.^{2}) load-bearing wooden studs.

The heat and moisture simulations show that the position of the aerogel blankets in relation to the thermal bridges is relevant. The different aerogel blanket walls had a large variation in the moisture performance; for some positions the moisture condition was much worse than for the corresponding position in the walls with conventional insulation.

Wall 3b is the aerogel blanket wall that has the best moisture performance in this study (shown in Figure 6). The wooden studs in the service gap and in the load-bearing layer are positioned in line and a homogeneous layer of aerogel is put on the outside of the studs, just behind the façade.

The worst wall layout was found to be wall 2a (shown in Figure 6), for which the wooden studs in the service gap and the load-bearing layer were alternated, with a homogeneous aerogel layer placed in between. This construction had a high mold growth potential, both in the outmost parts of the wall and on the inside of the vaportight barrier. The performance was much worse than the performance for corresponding positions in the walls with conventional insulation.

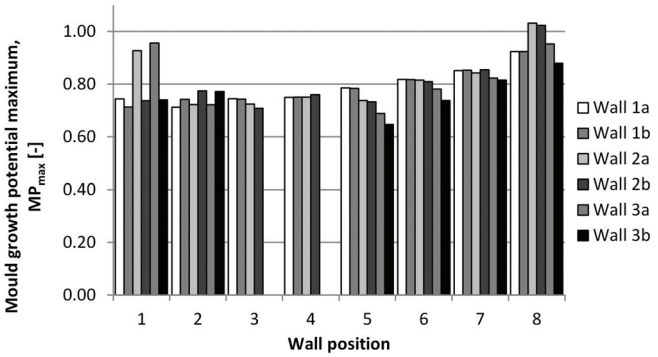

Figure 8 *Mold potential maximums for the different positions, shown in Figure 7, of the analyzed walls.*

ACKNOWLEDGMENTS

This work was a part of the project Homes for Tomorrow, mainly funded by FORMAS.

NOMENCLATURE

A	=	area, m^2 (ft^2)
D	=	vapor diffusivity, m^2/s
d	=	thickness, m (in. or ft)
G	=	mass flow, kg/s (lb/h)
K	=	thermal conductance, W/m^2/K (Btu/h/ft^2/°F)
MP	=	mold potential, dimensionless
P	=	pressure, Pa (mm Hg)
Q	=	heat flow, W (Btu/h)
RH	=	relative humidity, %
T	=	temperature, K or °C (°F)
U	=	thermal transmittance, W/m^2/K (Btu/h/ft^2/°F)
v	=	vapor content, kg/m^3 (lb/ft^3)
δ	=	permeability, kg/Pa/s/m (perm in.)
λ	=	thermal conductivity, W/m/K (Btu·in./h/ft^2/°F)
φ	=	relative humidity, dimensionless

Subscripts

a	=	air
aeb	=	aerogel blanket
crit	=	critical value
s	=	saturation
v	=	vapor

REFERENCES

Berge, A., and P. Johansson. 2012. Literature Review of High Performance Thermal Insulation (Report 2012:2), Department of Civil and Environmental Engineering, Chalmers University of Technology, Göteborg, Sweden.

COMSOL. 2013. COMSOL Multiphysics® 4.2b, Heat Transfer Module. COMSOL Inc.

CEN. 1994. Standard EN 823:1994, *Thermal insulation products for building applications – determination of thickness.* Brussels: European Committee for Standardization.

CEN. 2012. CEN Standard EN ISO 13788, *Hygrothermal performance of building components and building elements - Internal surface temperature to avoid critical surface humidity and interstitial condensation - Calculation methods.* Brussels: European Committee for Standardization.

Fricke, J., X. Lu, P. Wang, D. Büttner, and U. Heinemann. 1992. Optimization of monolithic silica aerogel insulants. *International Journal of Heat and Mass Transfer* 35(9):2305–2309.

Hukka E., and H.A. Viitanen. 1999. A mathematical model of mould growth on wooden material. *Wood Science and Technology* 33.

Johannesson, C. 1992. *Träbyggnadshandbok 3: Väggar* (*Wood Building Handbook 3: Walls*). Tryckeriteknik i Malmö AB, Malmö. (ISBN 91-85576-22-0)

Kistler, S.S. 1931. Coherent expanded aerogels. *Journal of Physical Chemistry* 36(1):52–64.

Petersson, B.-Å. 2009. *Tillämpad byggnadsfysik*, 4th ed. Lund: Studentlitteratur. (ISBN: 978-91-44-05817-7)

Pietruszka, B., J. Babinska, and R. Gerylo. 2012. Aerogel-based thermal insulation materials - structure and properties. *Proceedings of the 5th IBPC. International Building Physics Conference, Kyoto*, pp. 117–23.

Soleimani Dorcheh, A., and M. Abbasi. 2008. Silica aerogel: Synthesis, properties and characterization. *Journal Of Materials Processing Technology* 199(1–3):10–26.

Stepanian, C., G. Gould, and R. Begag. 2006. Aerogel composite with fibrous batting. Pat. No. US 7,504,346.

Swedish Government. 2013. Mål och åtgärder (Objectives and measures). www.regeringen.se Ansvarsområden > Miljö, energi och klimat > Klimat > Nationellt klimatarbete (available: 2013-01-17).

IBP. 2013. WUFI® 2D. Stuttgart: Fraunhofer IBP. www.wufi.com

Zirkelbach, D., T. Schmidt, H. Künzel, M. Kehrer, and C. Bludau. 2013. WUFI 2D Calculation example step by step. www.wufi.com > Downloads > WUFI 2D example [available: 2013-01-31].